

**Ferroelectric photovoltaic properties in doubly substituted
(Bi_{0.9}La_{0.1})(Fe_{0.97}Ta_{0.03})O₃ thin films**

R. K. Katiyar, Y. Sharma, D. Barrionuevo, S. Kooriyattil, S. P. Pavunny, J. S. Young, G. Morell, B. R. Weiner, R. S. Katiyar, and J. F. Scott

Citation: *Applied Physics Letters* **106**, 082903 (2015); doi: 10.1063/1.4908254

View online: <http://dx.doi.org/10.1063/1.4908254>

View Table of Contents: <http://scitation.aip.org/content/aip/journal/apl/106/8?ver=pdfcov>

Published by the [AIP Publishing](#)

Articles you may be interested in

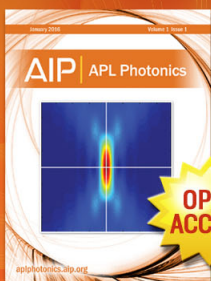
[Switchable photovoltaic and polarization modulated rectification in Si-integrated Pt/\(Bi_{0.9}Sm_{0.1}\)\(Fe_{0.97}Hf_{0.03}\)O₃/LaNiO₃ heterostructures](#)
Appl. Phys. Lett. **107**, 162904 (2015); 10.1063/1.4934665

[Oxygen vacancies induced switchable and nonswitchable photovoltaic effects in Ag/Bi_{0.9}La_{0.1}FeO₃/La_{0.7}Sr_{0.3}MnO₃ sandwiched capacitors](#)
Appl. Phys. Lett. **104**, 031906 (2014); 10.1063/1.4862793

[Ferroelectric polarization switching kinetics process in Bi_{0.9}La_{0.1}FeO₃ thin films](#)
J. Appl. Phys. **114**, 174101 (2013); 10.1063/1.4828880

[Photovoltaic characteristics in polycrystalline and epitaxial \(Pb_{0.97}La_{0.03}\)\(Zr_{0.52}Ti_{0.48}\)O₃ ferroelectric thin films sandwiched between different top and bottom electrodes](#)
J. Appl. Phys. **105**, 061624 (2009); 10.1063/1.3073822

[Ferroelectric properties, morphologies, and leakage currents of Bi_{0.97}La_{0.03}FeO₃ thin films deposited on indium tin oxide/glass substrates](#)
J. Appl. Phys. **104**, 076103 (2008); 10.1063/1.2975321



Launching in 2016!
The future of applied photonics research is here

**OPEN
ACCESS**

AIP | APL
Photonics

Ferroelectric photovoltaic properties in doubly substituted $(\text{Bi}_{0.9}\text{La}_{0.1})(\text{Fe}_{0.97}\text{Ta}_{0.03})\text{O}_3$ thin films

R. K. Katiyar,^{1,2,a)} Y. Sharma,^{1,2} D. Barrionuevo,^{1,2} S. Kooriyattil,^{1,2} S. P. Pavunny,^{1,2} J. S. Young,^{1,2} G. Morell,^{1,2} B. R. Weiner,^{1,3} R. S. Katiyar,^{1,2} and J. F. Scott⁴

¹Department of Physics, University of Puerto Rico, San Juan, Puerto Rico 00936, USA

²Institute for Functional Nanomaterials, University of Puerto Rico, San Juan, Puerto Rico 00931, USA

³Department of Chemistry, University of Puerto Rico, San Juan, Puerto Rico 00936, USA

⁴Cavendish Laboratory, Department of Physics, University of Cambridge, Cambridge CB0 3HE, United Kingdom

(Received 26 November 2014; accepted 4 February 2015; published online 23 February 2015)

Doubly substituted $[\text{Bi}_{0.9}\text{La}_{0.1}][\text{Fe}_{0.97}\text{Ta}_{0.03}]\text{O}_3$ (BLFTO) films were fabricated on Pt/TiO₂/SiO₂/Si substrates by pulsed laser deposition. The ferroelectric photovoltaic properties of ZnO:Al/BLFTO/Pt thin film capacitor structures were evaluated under white light illumination. The open circuit voltage and short circuit current density were observed to be ~ 0.20 V and ~ 1.35 mA/cm², respectively. The band gap of the films was determined to be ~ 2.66 eV, slightly less than that of pure BiFeO₃ (2.67 eV). The PV properties of BLFTO thin films were also studied for various pairs of planar electrodes in different directions in polycrystalline thin films.

© 2015 AIP Publishing LLC. [<http://dx.doi.org/10.1063/1.4908254>]

BiFeO₃ (BFO) is known to be a lead-free ferroelectric material with excellent ferroelectric properties, comparable to those of Pb(Zr,Ti)O₃.^{1–3} Recently, polarization-mediated photovoltaic properties in BFO films have been reported.^{4–7} Such photovoltaic effects arise differently to those of conventional p-n and Schottky junctions, which originate from the built-in field across depletion layers.⁸ Many research groups have reported that a site-engineering technique using various elements is effective in suppressing the significant leakage current observed often in BFO films.^{9–13} Under this context, we studied the photovoltaic (PV) effect in doped BFO, where Bi was replaced by La and Fe was replaced by higher-valence transition metals, such as Ti and Zr, for improving electrical properties.¹⁴ Among ferroelectrics, BFO has a large remnant polarization (Pr) and a rather small direct band gap (E_g) of 2.67 eV.^{15,16} Large optical absorption coefficients are expected for this material in visible light and thus make it a promising photovoltaic material.¹⁷ As mentioned above, doping of foreign atoms into BFO and/or fabricating a composite film with other single phase ferroelectric materials could be possible ways to overcome the leakage current effect on photovoltaic properties of ferroelectric PVs (FEPVs).¹⁸ The leakage current density in ferroelectrics corresponds to the dark current density or the dark conductivity in photovoltaics.¹⁹ In this paper, the effect of La and Ta codoping on the ferroelectric and photovoltaic properties of BFO films are presented. Moreover, the influence of electrode configuration on the photovoltaic response of ZnO:Al/ $[\text{Bi}_{0.9}\text{La}_{0.1}][\text{Fe}_{0.97}\text{Ta}_{0.03}]\text{O}_3$ (BLFTO)/Pt heterostructures was also investigated.

BLFTO films were deposited on Pt/TiO₂/SiO₂/Si and fused silica (FS) substrates using a conventional pulsed laser deposition (PLD) system equipped with a KrF excimer laser (Coherent Compex-Pro 201) operating at 248 nm wavelength. High quality and dense films were grown using a

constant laser energy of ~ 75 mJ/pulse on the BLFTO ceramic target, from the laser beam that is passed through an aperture to obtain a homogenous flat-top beam profile. The phase formation of the films was carried out at ~ 20 mTorr of oxygen pressure and ~ 760 °C substrate temperature allowing a film growth duration of ~ 1600 s at ~ 10 Hz pulse repetition rate. The thickness of the deposited films was measured to be ~ 350 nm. The top electrodes of ZnO:Al with an area of $\sim 3.14 \times 10^{-4}$ cm² were deposited on the BLFTO film by the same PLD system using a shadow mask to obtain solar cell structures. The phase formation of a crystalline structure of BLFTO thin film was determined by X-ray diffraction (XRD), performed on a Rigaku D/Max Ultima II X-ray diffractometer using a Cu K α source operated at a very low scan rate of 0.025°/min over the 2θ range of 20°–80°. Structural characterization of BLFTO thin film was carried out by Raman spectroscopy using T64000 spectrometer equipped with a triple grating monochromator and a Coherent Innova 70C Ar ion laser operating at 514.5 nm. The optical transmission spectra of the as grown samples on fused silica were measured by UV/Vis spectroscopy. The electrical properties of the devices were examined using an electrometer (Keithley model 2401) and ferroelectric nature of the film was measured by a Veeco Piezoforce Microscope (PFM) operated in contact mode. To characterize photovoltaic properties, illumination using a solar simulator operating at visible wavelength region (ABET Model 3000) with a power density of 100 mW/cm² was employed. The current density vs. voltage (J-V) characteristics was examined with and without light illumination. All measurements were performed at room temperature (RT).

XRD spectra (in log scale) showed in Fig. 1(a) confirmed that all major Bragg peaks corresponded to a rhombohedral structure with R3c space group and revealed the polycrystalline nature of the films. As shown in the inset of Fig. 1(a), the full width half maxima (FWHM) of the peak (110) at $2\theta \sim 31^\circ$ were determined to be ~ 0.2069 by Lorentzian fitting confirming a highly crystalline structure.

^{a)}Author to whom correspondence should be addressed. Electronic mail: rajesh_katiyar3006@yahoo.com.

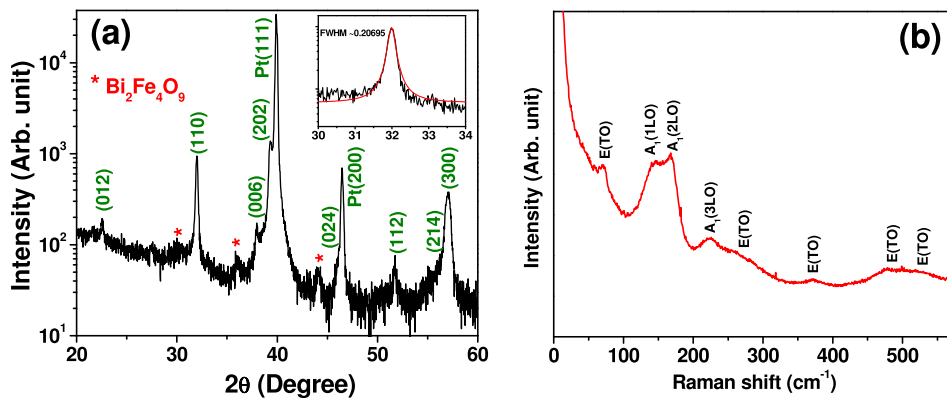


FIG. 1. (a) Room temperature XRD diffractograms of BLFTO films. FWHM calculated by Lorentzian fitting is given in inset. (b) Raman spectra of the polycrystalline thin films of BLFTO.

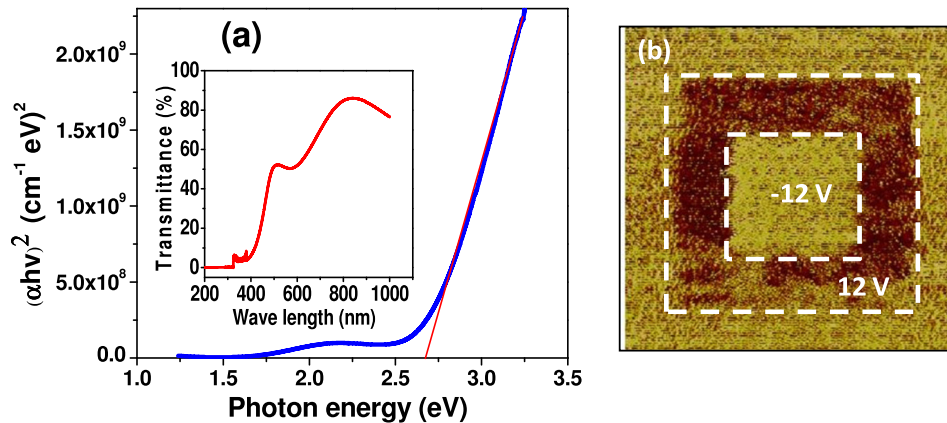


FIG. 2. (a) Modified Tauc's plot for the BLFTO sample for the determination of energy bandgap. Optical transmittance spectrum of 350 nm thick BLFTO film is displayed in the inset. The ferroelectric nature of the BLFTO films with an applied tip bias voltage of ± 12 V over a $100 \mu\text{m}^2$ area measured by piezoresponse force microscopy is shown in Fig. 2(b).

We identified the minor peaks near $2\theta = 30$ (002), 36 (022), and 44 (144) as those originated from orthorhombic mullite-type structure of $\text{Bi}_2\text{Fe}_4\text{O}_9$ with space group Pbam .²⁰ The factor group analysis for the rhombohedral structure with $R3c$ space group predicts 13 normal modes given by $\Gamma_{\text{Raman}} = 4A_1 + 9E$.²¹ Phase formation of BLFTO film was confirmed by Raman spectroscopy, where most of the phonon modes were identified in the $10\text{--}575 \text{ cm}^{-1}$ spectral window as shown in Figure 1(b). A representative spectral transmission curve of the BLFTO thin films is displayed in inset of Fig. 2(a). The sharp fall in transmission and disappearance of the interference fringes (due to interference at the air- and substrate-film interfaces) at the shorter wavelength is caused by the fundamental absorption in the films. It is worth mentioning that the hump observed in the spectra below 400 nm is due to an instrumental artifact observed during lamp switch at about 350–300 nm from a tungsten halogen lamp (Visible/near infra-red) to a deuterium lamp (UV) and is caused by a change in beam path between the background correction and sample measurement. Figure 2(a) illustrates the direct bandgap (E_g) estimation of BLFTO thin layer to be $\sim 2.66 \text{ eV}$ from a modified square law based bandgap calculations using the $(\alpha h\nu)^2$ vs $h\nu$ plots, by extrapolating the linear portion of the absorption to the X-axis where absorption coefficient becomes zero. This optical gap determined is very close to the reported E_g of 2.67 eV for BFO films. The BLFTO film shows a large optical absorption at or above 2.5 eV (at or below $\sim 500 \text{ nm}$) even though $h\nu$ is slightly below the band gap of 2.66 eV, suggesting that the BLFTO film absorbs more than 50% of the incident photon energy at this region as shown in the inset of Fig. 2(a).

Pure BFO films often show large leakage currents and poor hysteresis loops owing to the valence fluctuation of Fe ions and/or Bi or O deficiencies. In fact, it is not easy to reproducibly obtain excellent ferroelectric properties of pure BFO films.²² An improved ferroelectric characteristic of thin films was achieved by co-doping pure BFO and was confirmed by PFM. The square pattern of two opposite polarization domains can be seen from the contrasting areas, due to the application of a tip bias of $\pm 12 \text{ V}$, as shown in Fig. 2(b). The

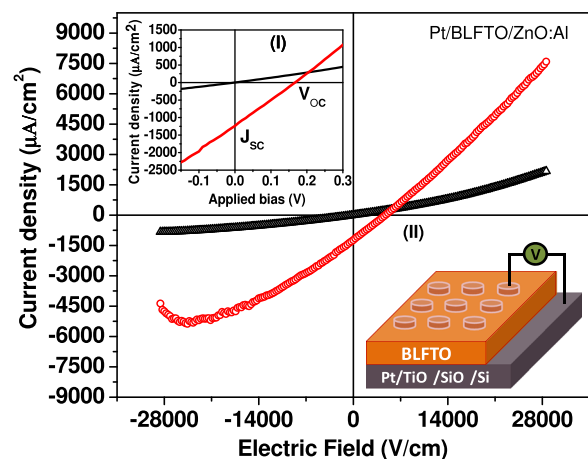


FIG. 3. Current density as a function of applied bias voltage for the Pt/BLFTO/ZnO:Al heterostructures obtained under illumination (energy density of $\sim 100 \text{ mW/cm}^2$). The inset corresponds to the enlarged region around the origin and identifies the values for V_{OC} and J_{SC} . (Legend: red = under illumination and black = under dark) and schematic diagram of Pt/BLFTO/ZnO:Al device.

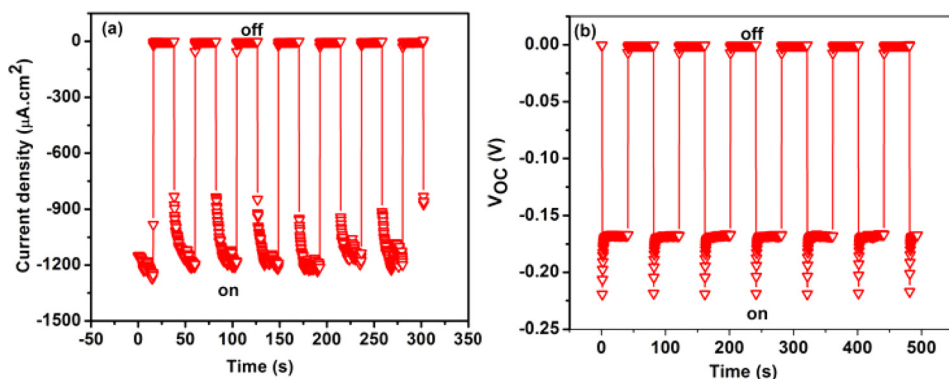


FIG. 4. The J_{sc} (a) and V_{oc} (b) as a function of time in Pt/BLFTO/ZnO:Al heterostructures under illumination (energy density of ~ 100 mW/cm²).

domain switching behavior could be a signature of a ferroelectric nature of as grown film.^{23,24}

The photo-excited carrier transport and photovoltaic measurements were performed for the device. Figure 3 displays J-E plots with (red curve) and without (black curve) illumination for the BLFTO cells. For the photovoltaic measurements, a voltage of ± 1 V was applied to the cells under dark conditions and then illuminated conditions, in top-to-bottom electrode configuration. The magnified J-V curves around the origin and the schematic diagram of ZnO:Al/BLFTO/Pt device are shown in the inset I and II of Figure 3, respectively. It was found that the cell shows a photovoltaic effect, resulting in a finite short circuit current density (J_{sc}) and open circuit voltage (V_{oc}). We observed enhanced photovoltaic response in BLFTO sample as compared to Zr and Ti co-doped BFO sample. The leakage current density measured was almost two orders of magnitude less in BLFTO.¹⁴ Based on the previous studies, pure BFO showed a leakage current density of $\sim 10^{-2}$ A/cm² (at 1 V),²⁵ which is one order higher as compared to the observed value of $\sim 10^{-3}$ A/cm² (at 1 V) in our BLFTO film. The dark J-V curve of the BLFTO cell shows a high resistance state, irrespective of the voltage. The photovoltaic features are completely different from the conventional features of a p-n-diode, pin-diode, or Schottky-diode solar cells without any voltage-sweep hysteresis. The conventional photovoltaic property is based on the dark diode-like J-V behavior, and the J-V curve is shifted downward with an increase in illumination intensity. The results shown in Fig. 3 indicate that the as-grown BLFTO films exhibit a photovoltaic effect.

Thus far, two models have been proposed for the switchable polarization-induced photovoltaic effect. Yang *et al.*²⁶ reported that a high-quality BFO film with coplanar electrodes shows an “above band gap” photovoltage proportional to the number of domains and proposed that the photo-excited carriers are separated at nano-scale steps of the electrostatic potential at ferroelectric domain walls. Lee *et al.*²⁷ reported that an epitaxial BFO cell sandwiched by top and bottom electrodes shows a below-band gap photovoltage, and they proposed that the photo-excited carriers are separated by macroscopic polarization over the whole film thickness. The latter mechanism can be ascribed to the depolarization field, which results from the incomplete screening of ferroelectric polarization by the electrodes. A simple consideration of the polarity of the photovoltaic effect will tell us which mechanism is valid.²⁸ Confirmation of the polarity of V_{oc} and J_{sc} of the present cells after the application of the electric field revealed that the present photovoltaic effect is ascribed to the depolarization effect due to the incomplete screening.

To facilitate the repeatability of our results, we verified the photovoltaic effect of the BLFTO cell as a function of time at zero bias and measured the short circuit current (J_{sc}) separately (over a total time of 350 s with 40 s on/off intervals). The photo-response of BLFTO capacitors is shown in Fig. 4(a). The J_{sc} increases rapidly when exposed to light and finally saturates at a value of ~ 1.35 mA/cm². When the light is turned off, the J_{sc} decreases rapidly over ~ 120 ms to reach its original state. The V_{oc} of the BLFTO cell was also studied as a function of time with periodic exposure of light for a period of 40 s, Fig. 4(b). The V_{oc} increases rapidly on exposure

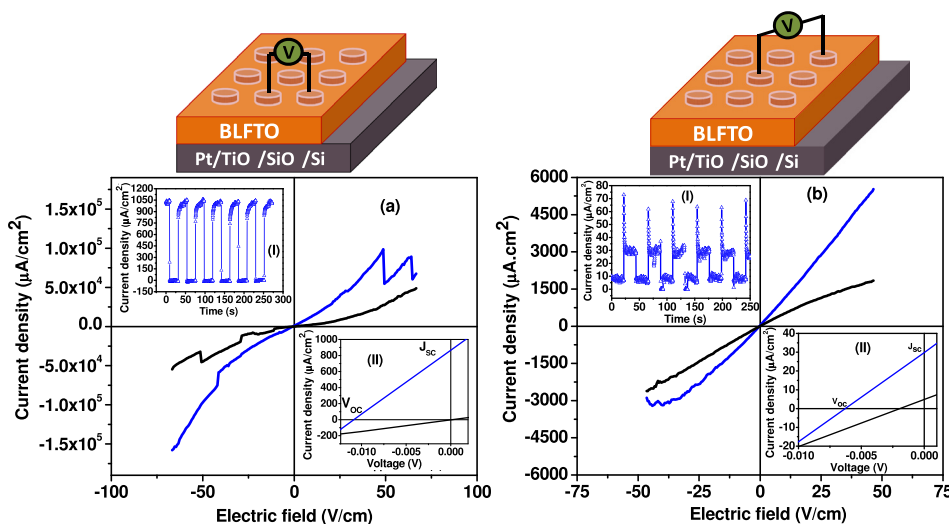


FIG. 5. The photovoltaic effect measured in planar configuration of electrodes (a) ~ 150 μm (b) ~ 215 μm under illumination (energy density of ~ 100 mW/cm²).

to light and saturates at a value of ~ 0.20 V. When the light is turned off, the V_{oc} decreases over ~ 175 ms to reach its original state. Further, we observed stable photoresponses [insets I of Figures 5(a) and 5(b)] and considerable amounts of J_{sc} and V_{oc} [insets II of Figures 5(a) and 5(b)] in planar configuration of electrodes that revealed the photovoltaic effect in the BLFTO film. However, J_{sc} and V_{oc} were found to vary between various pairs of planar electrodes as the direction of polarization is not the same between them in polycrystalline thin films.

In conclusion, the polycrystalline thin films of BLFTO were grown by PLD. The optical measurements on the film confirmed the direct band gap to be ~ 2.66 eV, very close to that in pure BFO. The ferroelectric nature of the film was confirmed by PFM. The device showed a PV effect with improved J_{sc} and V_{oc} of ~ 1.35 mA/cm² and ~ 0.20 V across top and bottom electrodes under intense illumination. The performance of the device showed reliable repeatability over time and the PV effect was studied for various pairs of planar electrodes in different directions.

This work was supported by the DOE-EPSCoR Grant No. DE-FG02-08ER46526. Acknowledgment is also due to NSF Grant No. #1002410 for providing fellowships to R.K.K., D.B., and J.S.Y.

- ¹J. Wang, J. B. Neaton, H. Zheng, V. Nagarajan, S. B. Ogale, B. Liu, D. Viehland, V. Vaithyanathan, D. G. Schlom, U. V. Waghmare *et al.*, *Science*, **299**, 1719 (2003).
- ²J. Wang, H. Zheng, Z. Ma, S. Prasertchoug, M. Wuttig, R. Droopad, J. Yu, K. Eisenbeiser, and R. Ramesh, *Appl. Phys. Lett.* **85**, 2574 (2004).
- ³D. Lebeugle, D. Colson, A. Forget, and M. Viret, *Appl. Phys. Lett.* **91**, 022907 (2007).
- ⁴A. Z. Simoes, L. S. Cavalcante, C. S. Riccardi, J. Varela, and E. Longo, *Curr. Appl. Phys.* **9**, 520 (2009).
- ⁵K. Sone, H. Naganuma, T. Miyazaki, T. Nakajima, and S. Okamura, *Jpn. J. Appl. Phys.* **49**, 09MB03 (2010).
- ⁶S. R. Basu, L. W. Martin, Y. H. Chu, M. Gajek, R. Ramesh, R. C. Rai, X. Xu, and J. L. Musfeldt, *Appl. Phys. Lett.* **92**, 091905 (2008).
- ⁷R. K. Katiyar, A. Kumar, G. Morell, J. F. Scott, and R. S. Katiyar, *Appl. Phys. Lett.* **99**, 092906 (2011).

- ⁸D. Daranciang, M. J. Highland, H. Wen, S. M. Young, N. C. Brandt, H. Y. Hwang, M. Vattilana, M. Nicoul, F. Quirin, J. Goodfellow *et al.*, *Phys. Rev. Lett.* **108**, 087601 (2012).
- ⁹R. K. Katiyar, P. Misra, S. Sahoob, G. Morell, and R. S. Katiyar, *J. Alloys Compd.* **609**, 168 (2014).
- ¹⁰H. Naganuma, J. Miura, and S. Okamura, *Appl. Phys. Lett.* **93**, 052901 (2008).
- ¹¹B. Yu, M. Li, Z. Hu, L. Pei, D. Guo, X. Zhao, and S. Dong, *Appl. Phys. Lett.* **93**, 182909 (2008).
- ¹²V. S. Puli, D. K. Pradhan, R. K. Katiyar, I. Coondoo, N. Panwar, P. Misra, D. B. Chrisey, J. F. Scott, and R. S. Katiyar, *J. Phys. D: Appl. Phys.* **47**, 075502 (2014).
- ¹³J. Junquera and P. Ghosez, *Nature* **422**, 506 (2003).
- ¹⁴R. K. Katiyar, Y. Sharma, P. Misra, V. S. Puli, S. Sahoo, A. Kumar, J. F. Scott, G. Morell, B. R. Weiner, and R. S. Katiyar, *Appl. Phys. Lett.* **105**, 172904 (2014).
- ¹⁵B. Eom, R. J. Cava, R. M. Fleming, J. M. Philips, R. B. Dover, J. H. Marshall, J. W. P. Hsu, J. J. Krajewski, and W. F. Peck, Jr., *Science* **258**, 1766 (1992).
- ¹⁶S. Y. Yang, L. W. Martin, S. J. Byrnes, T. E. Conry, S. R. Basu, D. Paran, L. Reichertz, J. Ihlefeld, C. Adamo, A. Melville *et al.*, *Appl. Phys. Lett.* **95**, 062909 (2009).
- ¹⁷T. L. Qu, Y. G. Zhao, D. Xie, J. P. Shi, Q. P. Chen, and T. L. Ren, *Appl. Phys. Lett.* **98**, 173507 (2011).
- ¹⁸Y. Wang, G. Xu, L. Yang, Z. Ren, X. Wei, W. Weng, and P. Du, *Mater. Lett.* **62**, 3806 (2008).
- ¹⁹J. Zhang, X. Su, M. Shen, Z. Dai, L. Zhang, X. He, W. Cheng, M. Cao, and G. Zou, *Sci. Rep.* **3**, 2109 (2013).
- ²⁰JCPDS# 25-0090 and Y. Du, Z. X. Cheng, S. X. Dou, and X. L. Wang, *Mater. Lett.* **64**, 2251 (2010).
- ²¹N. M. Murari, R. Thomas, R. E. Melgarejo, S. P. Pavunny, and R. S. Katiyar, *J. Appl. Phys.* **106**, 014103 (2009).
- ²²S. Y. Yang, F. Zavaliche, L. Mohaddes-Ardabili, V. Vaithyanathan, D. G. Schlom, Y. J. Lee, Y. H. Chu, M. P. Cruz, Q. Zhan, T. Zhao, and R. Ramesh, *Appl. Phys. Lett.* **87**, 102903 (2005).
- ²³S. H. Baek, H. W. Jang, C. M. Folkman, Y. L. Li, B. Winchester, J. X. Zhang, Q. He, Y. H. Chu, C. T. Nelson, M. S. Rzchowski *et al.*, *Nat. Mater.* **9**, 309 (2010).
- ²⁴R. K. Katiyar, P. Misra, F. Mendoza, G. Morell, and R. S. Katiyar, *Appl. Phys. Lett.* **105**, 142902 (2014).
- ²⁵S.-H. Jo, S.-G. Lee, and Y.-H. Lee, *Nanoscale Res. Lett.* **7**, 54 (2012).
- ²⁶S. Y. Yang, J. Seidel, S. J. Byrnes, P. Shafer, C.-H. Yang, M. D. Rossell, P. Yu, Y.-H. Chu, J. F. Scott, J. W. Ager *et al.*, *Nat. Nanotechnol.* **5**, 143 (2010).
- ²⁷D. Lee, S. H. Baek, T. H. Kim, J. G. Yoon, C. M. Folkman, C. B. Eom, and T. W. Noh, *Phys. Rev. B* **84**, 125305 (2011).
- ²⁸R. R. Mehta, B. D. Silverman, and J. T. Jacobs, *J. Appl. Phys.* **44**, 3379 (1973).